Deep–Sea Research I 164 (2020) 103341

Contents lists available at ScienceDirect

Deep-Sea Research Part I

journal homepage: http://www.elsevier.com/locate/dsri

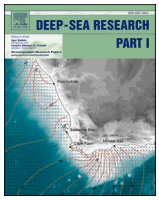

North Pacific deep-sea ecosystem responses reflect post-glacial switch to pulsed export productivity, deoxygenation, and destratification

Christina L. Belanger [a,*], Sharon [a], Jianghui Du [b,c], Calie R. Payne [a], Alan C. Mix [b]

[a] Department of Geology and Geophysics, Texas A&M University, College Station, TX, 77843, USA
[b] College of Earth, Ocean, and Atmospheric Sciences, Oregon State University, Corvallis, OR, 97331, USA
[c] Now at Institute of Geochemistry and Petrology, Department of Earth Sciences, ETH Zürich, Clausiusstrasse 25, 8092, Zürich, Switzerland

ARTICLE INFO

Keywords:
Export productivity
Glacial-interglacial
Benthic foraminifera
Dysoxia
Phytodetritus

ABSTRACT

Deep-sea ecosystems are highly sensitive to changes in organic matter export and oxygenation driven by climate change. Here we document past ecological changes in benthic foraminiferal assemblages indicative of deglacial changes in deep-sea oxygenation and the character of organic matter fluxes from sedimentary records retrieved at intermediate (692 m) and abyssal (3667m) depths in the Gulf of Alaska. Constrained multivariate ordination combining faunal and geochemical data over the past ~22,000 years distinguishes the impacts of pulsed productivity, which exports carbon to the abyss, from extreme dysoxia across the deglacial warming transition. At both depths, opportunistic species are more prevalent in interglacial conditions, reflecting higher pulsed organic matter export to the seafloor developed in response to warming and reduced sea-ice cover. Benthic foraminiferal species tolerant of low-oxygen conditions increased in abundance during the deglacial transition at both intermediate and abyssal depths. Authigenic trace metals reveal sulfidic sedimentary conditions indicative intermittent anoxia, but only at intermediate-depths. Benthic foraminiferal richness and evenness are also highest during this deglacial low-oxygen interval, likely due to high food availability. Last Glacial Maximum faunas were distinctly different at the two sites, consistent with a more stratified deep Pacific, but the faunas become more similar during Holocene time, suggesting destratification of the abyss during deglaciation. These ecosystem responses support that carbon fluxes increased during warm intervals in subpolar regions and underscores the importance of considering the effects of transient biological blooms on paleoceanographic interpretations and in model projections of future deep carbon export.

1. Introduction

The deep sea contains the largest ecosystems on Earth and plays a significant role in global carbon cycling by sequestering carbon transferred by the ocean's biological carbon pump (Honjo et al., 2014). Although the deep sea has long been thought to be more stable than surface-ocean or terrestrial environments, abyssal ecosystems are hypothesized to be sensitive to change via climate's influence on primary productivity and ocean oxygenation (Smith et al., 2009; Rogers, 2015). For example, future warming of the surface ocean is projected to increase stratification and inhibit vertical mixing of nutrients, resulting in a net reduction of global average export productivity (Bopp et al., 2013). However, regional disagreements occur at high latitudes and in some high productivity regions due, in part, to how models address micronutrient controls, different classes of phytoplankton, and controls on rates of subsurface carbon remineralization (Steinacher et al., 2010; Flombaum et al., 2020). Some models forecast up to a 60% increase in the flux of particulate organic matter to bathyal and abyssal regions of the Arctic Ocean and Southern Ocean due to increased primary productivity during longer ice-free periods (Sweetman et al., 2017). The potential impacts of changing productivity on the abyss also remains uncertain because export fluxes may be decoupled from primary productivity (Bopp et al., 2005; Moran et al., 2010; Lopes et al., 2015; Sweetman et al., 2017). For example, oxygen consumption from carbon remineralization a few hundred meters below the euphotic zone varies much less between the subtropical and subpolar North Pacific than does primary productivity (Emerson, 2014), suggesting carbon exports are relatively insensitive to climate change, whereas studies of the Arctic Ocean project greater increases in export production than in primary production with future climate change (Lavoie et al., 2010). Pulsed

* Corresponding author.
E-mail address: Christina.Belanger@tamu.edu (C.L. Belanger).

https://doi.org/10.1016/j.dsr.2020.103341
Received 15 January 2020; Received in revised form 27 April 2020; Accepted 13 June 2020
Available online 3 July 2020
0967-0637/© 2020 Elsevier Ltd. All rights reserved.

export production associated with biological blooms is thought to be more effective at reaching the deep sea than is steady export in which most organic matter is remineralized at shallow to intermediate depths (Smith et al., 2018). Thus, elucidating how large-scale climate change affects the pattern of carbon export is also important for understanding variations in the oceanic carbon cycle and forecasting climate's future impacts on deep-sea benthic ecosystems and carbon storage.

Paleoecological records of benthic marine communities provide an opportunity to observe and better understand the impacts of climate-driven impacts on the deep sea. Here we examine the ecological responses of benthic foraminiferal faunas to deglaciation at two sites from the Gulf of Alaska (GoA) over the past 22 ka at multi-centennial resolution (Fig. 1). In the GoA, regional deglacial warming of the sea surface started at ~17 ka and accelerated from 15.2 to 14.7 ka. After a cooling interval from ~13.5–12 ka, warming recommenced at ~12 ka and accelerated at 11 ka (Praetorius et al., 2015). Lithological evidence from the intermediate-depth site indicates a change from fluctuating glacial conditions to a period of increased meltwater discharge at ~19 ka (Penkrot et al., 2018), consistent with the early phases of deglaciation elsewhere in the northern hemisphere. At ~14.5 ka, the lithology transitions abruptly from glacially-derived diamict to laminated hemipelagic mud as the Bering Glacier retreats onshore (Davies et al., 2011; Penkrot et al., 2018).

Hypoxic events are evident in both laminated structures and authigenic redox-sensitive trace metals (U and Mo) at intermediate depths in the Gulf of Alaska in the intervals 14.7–12.9 ka and 11.5–10.5 ka, plausibly associated with higher productivity (Barron et al., 2009; Davies et al., 2011; Addison et al., 2012; Praetorius et al., 2015). However, models of productivity responses to future climate change (Bopp et al., 2013), interseasonal observations from modern settings (Smith et al., 2018), and data from paleoceanographic records (Lopes et al., 2015), suggest that primary productivity may be decoupled from export productivity in some circumstances, which may be further decoupled from opal and carbon burial (Arndt et al., 2013; Chase et al., 2015). This decoupling can lead to disagreement among estimates of past carbon flux to the seafloor because those estimates often rely on different parts of the carbon cycle. For example, some estimates of carbon flux based on isotopic tracers of particle scavenging in the subpolar North Pacific imply higher organic fluxes during interglacial (warmer) intervals than during glacial (colder) times (Costa et al., 2018), however estimates based on organic carbon burial rates in the same region imply lower organic fluxes during interglacial (or warmer) times (Cartapanis et al., 2016). Assessments based on the opal and organic content of marine sediment in the NW Pacific also suggest lower biogenic fluxes during warmer (interglacial) times (Ohkushi et al., 2018). This contrasts, however, with nitrogen isotope evidence suggesting lower upwelling and lower productivity in the Bering Sea and North Pacific during glacial intervals (Worne et al., 2019). Further, the correlation between various productivity indices and biogenic burial fluxes vary across the Subarctic North Pacific, warning against the interpretation of burial fluxes in terms of paleoproductivity in this region (Serno et al., 2014).

To elucidate the impact of enhanced productivity on ocean deoxygenation and seafloor environments, it is essential to distinguish among carbon export that is primarily remineralized in the upper ocean and that which reaches the deep seafloor. Benthic foraminifera, which reside at or within centimeters of the sediment-water interface, can record the magnitude and character of carbon fluxes to the seafloor via changes in species composition and ecological structure. This group is particularly well-preserved in GoA sediments and high sedimentation rates yield detailed records of change, allowing us to examine deep-sea benthic ecological responses to climate change in the region. In contrast to earlier GoA data on just a few benthic taxa (Praetorius et al., 2015), we analyze the full benthic foraminiferal species diversity, which allows us to distinguish ecosystem responses to changing oxygen levels and to export productivity. If organic carbon fluxes to the seafloor increased after the Last Glacial Maximum, then we would expect post-glacial increases in the abundances of benthic foraminiferal species associated with fluxes of fresh phytodetritus or with high accumulations of less labile organic matter, depending on whether organic carbon increased via pulsed delivery or steady rain. We would also expect changes in ecological structure consistent with higher food availability including increased richness (number of species) and evenness (the similarity in relative abundances among species) relative to times of greater food stress (McCallum et al., 2015; Sweetman et al., 2017).

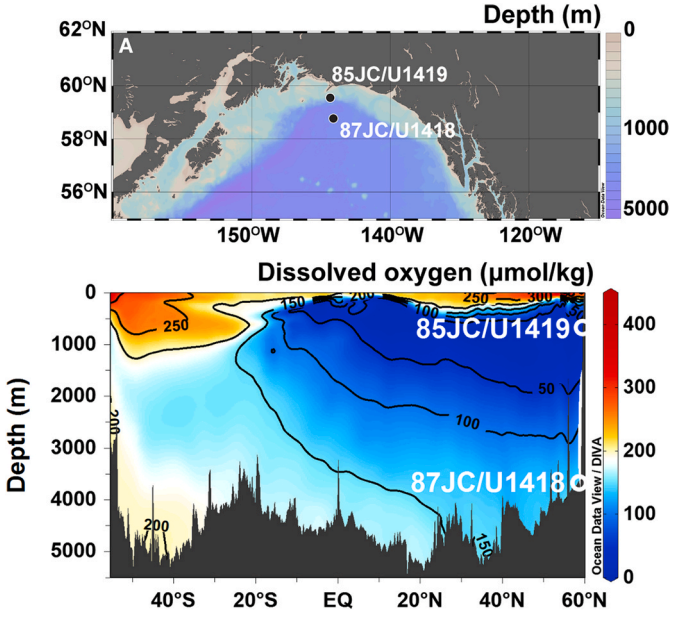

Fig. 1. A. Location map showing the location on the slope (U1419/85JC) and abyssal (U1418/87JC) sites in the Gulf of Alaska. B. Meridional cross section of the oxygen concentration in the modern Eastern Pacific Ocean, showing location of core sites with respect to the oxygen minimum zone. Data are from GLODAPv2.2019 (Olsen et al., 2016).

2. Methods

2.1. Study site and sampling

Integrated Ocean Drilling Program (IODP) Site U1419 and its co-located site-survey core EW0408-85JC underlie North Pacific Intermediate Water (NPIW) at 692 m water depth in the modern upper oxygen minimum zone (hereafter intermediate-depth site), while IODP Site U1418 and its associated site-survey core EW0408-87JC underlie Pacific Deep Water (PDW) at 3677 m water depth (hereafter abyssal site). Samples from U1419 and EW0408-85JC (intermediate site) and from U1418 and EW0408-87JC (abyssal site) were integrated using their respective age models, which are based on reservoir-corrected radiocarbon ages from planktonic foraminifera and tephrochronology (Davies-Walczak et al., 2014; Praetorius et al., 2015; Du et al., 2018). Samples were 2–3 cm wide (5–40 cc) depending on anticipated sedimentation rates and availability of material. Geochemical and faunal data were obtained from the same samples allowing direct comparisons among different proxies. At the intermediate-depth site, we analyzed 149 samples with a median sampling spacing of ~118 years. At the abyssal site, we analyzed 37 samples with a median sample spacing of ~310 years. All sample depths, assigned ages and data used herein are in Appendix A.

2.2. Redox-sensitive metal analyses

We use the redox-sensitive metals Molybdenum and Uranium,

normalized to Aluminum, as proxies for low-oxygen conditions. Mo accumulates in sediments at oxygenation values < 0.45 ml/L (Zheng et al., 2000), and thus, is a proxy for dysoxic (<0.5 ml/L O_2) conditions. Uranium begins accumulating during suboxic (0.5–1.4 ml/L O_2) conditions, thus, becomes enriched in sediments under less severe low-oxygen conditions than Mo (Tribovillard et al., 2006; McManus et al., 2006).

Freeze-dried bulk sediment samples (~50–100 mg) were digested in a CEM MARS-6 microwave oven using a mixture of HF–HCl–HNO_3 according to the established procedure at Oregon State University (Muratli et al., 2012). Aluminum was analyzed using ICP-OES in the W.M. Keck Collaboratory for Plasma Spectrometry of Oregon State University. Repeatedly digestion and analysis of the marine sediment reference material PACS-2 yield an Al concentration of 6.45 ± 0.16 (1σ, n = 58) wt %, which agrees well with the certified value of 6.62 ± 0.16 (1σ) wt%. Procedural blanks of total digestion were negligible (<0.1%) for Al. Repeated digestion and analysis of an in-house marine sediment standard yield long-term (over 3 years) reproducibility (1 relative standard deviation, n = 57) of ~2% of measured values for Al.

Molybdenum and Uranium were analyzed on a quadrupole ICP-MS in the same laboratory. Instrumental drifts were monitored and corrected for by spiking samples, calibration standards and blanks with internal standards (^{103}Rh and ^{209}Bi). Procedural blanks of total digestion were corrected for and were 0.8 ± 0.3% for Mo and 0.03 ± 0.01% for U. Repeated digestion and analysis of PACS-2 yield a Mo concentration of 5.70 ± 0.23 (1σ, n = 58) ppm, which agrees well with the certified value of 5.43 ± 0.14 (1σ) ppm. To calibrate U concentrations, we repeatedly digested the USGS certified rock materials AGV-1, which resulted in U concentration of 1.900 ± 0.049 (1σ, n = 3) ppm in agreement with the reference values of 1.903 ± 0.010 ppm (Jochum et al., 2016). Repeated digestion and analysis of an in-house marine sediment standard yield long-term (over 3 years) reproducibility (1 relative standard deviation, n = 57) of ~4% of measured values for Mo and of ~6% of measured values for U. Mo and U were normalized by using Element/Aluminum ratio to distinguish authigenic excess relative to terrigenous inputs (Muratli et al., 2010; Cartapanis et al., 2011). This normalization is however not essential given that Al and Ti concentrations, commonly used elements for lithogenic normalization, at both sites changed very little (<5%) in the studied interval, indicating nearly constant lithogenic background such that the variabilities of redox metal concentrations are almost entirely due to authigenic accumulation.

2.3. Stable isotope analyses

Stable isotope measurements were made on the planktonic foraminifer *Neogloboquadrina pachyderma* (sinistral) in the >125 μm size fraction after ultrasonic cleaning in methanol followed by an ultrasonic rinse in deionized water and drying at <50^{O}C. All measurements were made at the Oregon State University College of Earth Ocean and Atmospheric Sciences Stable Isotope Mass Spectrometer Facility using a Kiel-III carbonate preparation device connected to a Thermo-Finnigan MAT-252 mass spectrometer. Values are corrected to the PDB scale using both an in-house standard and the US National Institute of Standards and Technology RM8522 (NBS-19) standard. δ^{18}O and δ^{13}C external precision on standards is 0.03 and 0.02 permil (±1 standard deviation), respectively.

2.4. Faunal analyses

For benthic foraminiferal faunal analyses, samples were disaggregated in deionized water and wet-sieved at 63 μm. The coarse fraction (>63 μm) was split using a microsplitter to obtain at least 150 benthic foraminifers, although sample sizes as low as 50 individuals were included in samples where benthic foraminifera were less abundant or sample volume was small. While some studies recommend 300 individuals for statistical analyses of diversity metrics (Buzas, 1990), assemblage compositions are stable with as few as 58 individuals (Forcino et al., 2015). Samples with <300 individuals do not systematically differ in the ecological metrics we calculate below from those with larger counts (Appendix A).

Benthic foraminiferal responses to low oxygen can be confounded with responses to increased organic matter availability because organic-loving species often tolerate low-oxygen conditions (Jorissen et al., 2007). Here, we separate these effects using a distance-based redundancy analysis (RDA), which summarizes faunal variation associated with constraining environmental variables and produces one constrained axis for each constraining variable (Legendre and Anderson, 1999). Data from both the intermediate and abyssal site are analyzed together in the same RDA such that axes scores for each site are on the same scale. For ordination analysis, species counts were converted to relative abundances and samples related using the Bray-Curtis dissimilarity method, which is typically used in ecological studies (Legendre and Anderson, 1999; Borcard et al., 2018). Species that were not present in more than one sample or that comprised less than 2% of the assemblage in at least one sample were removed prior to ordination analysis to reduce noise.

Constraining variables (Mo/Al, U/Al, δ^{13}C and δ^{18}O) were z-score transformed prior to analysis, thus the resulting scores of the constraining variables are on the same unitless scale. Constraining the ordination to these co-registered geochemical proxies illuminates the components of faunal variation associated with each environmental factor on constrained axes and further separates out the remaining faunal variation associated with site differences unrelated to the environmental constraints on unconstrained axes.

We then use the known environmental preferences of species strongly associated with each axis of variation, such as their affiliation with different types of organic matter fluxes, to infer further ecological and environmental changes associated with the constrained environmental factors. We also use benthic foraminiferal species with published oxygen tolerances to corroborate our environmental interpretation of RDA axes. We define dysoxic indicators as those with a lowermost oxygen tolerance of 0.1 ml/L O_2 or less and suboxic indicators as those with a lowermost oxygen tolerance between 0.1 and 0.5 ml/L O_2 following Ohkushi et al. (2013) and Tetard et al. (2017) (Appendix A). RDA analyses were performed using the capscale function in the R programming package "vegan" (Oksanen et al., 2017). Only samples with data for all constraining variables are included in the analysis. Variance inflation factor (VIF) for all constraining variables is less than 5, thus multicollineary should not affect our analyses. VIF was calculated using the vif function in the HH package in R (Heiberger, 2018).

Species richness was calculated as the average number of species in a complete sample after 100 iterations of rarefaction to 50 individuals, the lowest number of individuals in any one sample, using the rarefaction function in the vegan package of the R programming language (Oksanen et al., 2017). The evenness of the abundance distribution was quantified using the probability of interspecific encounter (PIE) using the Hurlbert_PIE function in the paleotree package in R (Bapst, 2012).

3. Results and discussion

3.1. Environmental change at intermediate depth and abyssal sites

Deglacial deoxygenation has been previously recognized at intermediate depths in GoA using redox sensitive authigenic metals (excess Mo and excess U relative to crustal abundance) and selected benthic foraminiferal indicator taxa (Barron et al., 2009; Davies et al., 2011; Addison et al., 2012; Praetorius et al., 2015). The higher resolution redox metal data presented here add detail related to the transition and extends to deeper water depths.

Increasing U/Al, indicative of reduced oxygen penetration into seafloor sediments (Tribovillard et al., 2006; McManus et al., 2006), increases in our GoA records beginning at ~16.5 ka suggesting suboxic

conditions developed and persisted until 10.5 ka (Fig. 2). At the intermediate-depth site, U/Al is also elevated between ~6.2 ka and ~9 ka suggesting a return to suboxic conditions during the early Holocene, however these U/Al values are lower than during the deglacial interval. At the abyssal site, U/Al is generally elevated between 16.5 and 10.5 ka relative to glacial values. Thus, this new data indicates contemporaneous reduction of oxygen at both sites from ~16.5 to 10.5 ka, albeit with higher U/Al values in discrete events at the intermediate-depth site. These low oxygen conditions during the deglacial interval are apparent despite increases in abyssal circulation rate (Du et al., 2018) and reduced benthic-planktic age differences during the low oxygen events (Davies-Walczak et al., 2014).

Although Mo can accumulate as both oxides and sulfides, high enrichments of Mo are generally indicative of sulfidic environments in which oxygen is absent in porewaters (McManus et al., 2006; Scott and Lyons, 2012). In GoA, Mo/Al is low during glacial and interglacial intervals at both abyssal and intermediate depth sites (Fig. 2). During the deglacial interval, Mo/Al values are high during the two known dysoxic (<0.5 ml/L O_2) intervals at the intermediate-depth site (approximately aligned with the Bølling-Allerød warm event, ~15–13 ka, and the early Holocene, 11.5–10.5 ka; Praetorius et al., 2015), but remain low at the abyssal site, indicating that deglacial deoxygenation was more extreme at shallower depths.

Planktonic foraminiferal stable isotope records ($\delta^{13}C$ and $\delta^{18}O$) from

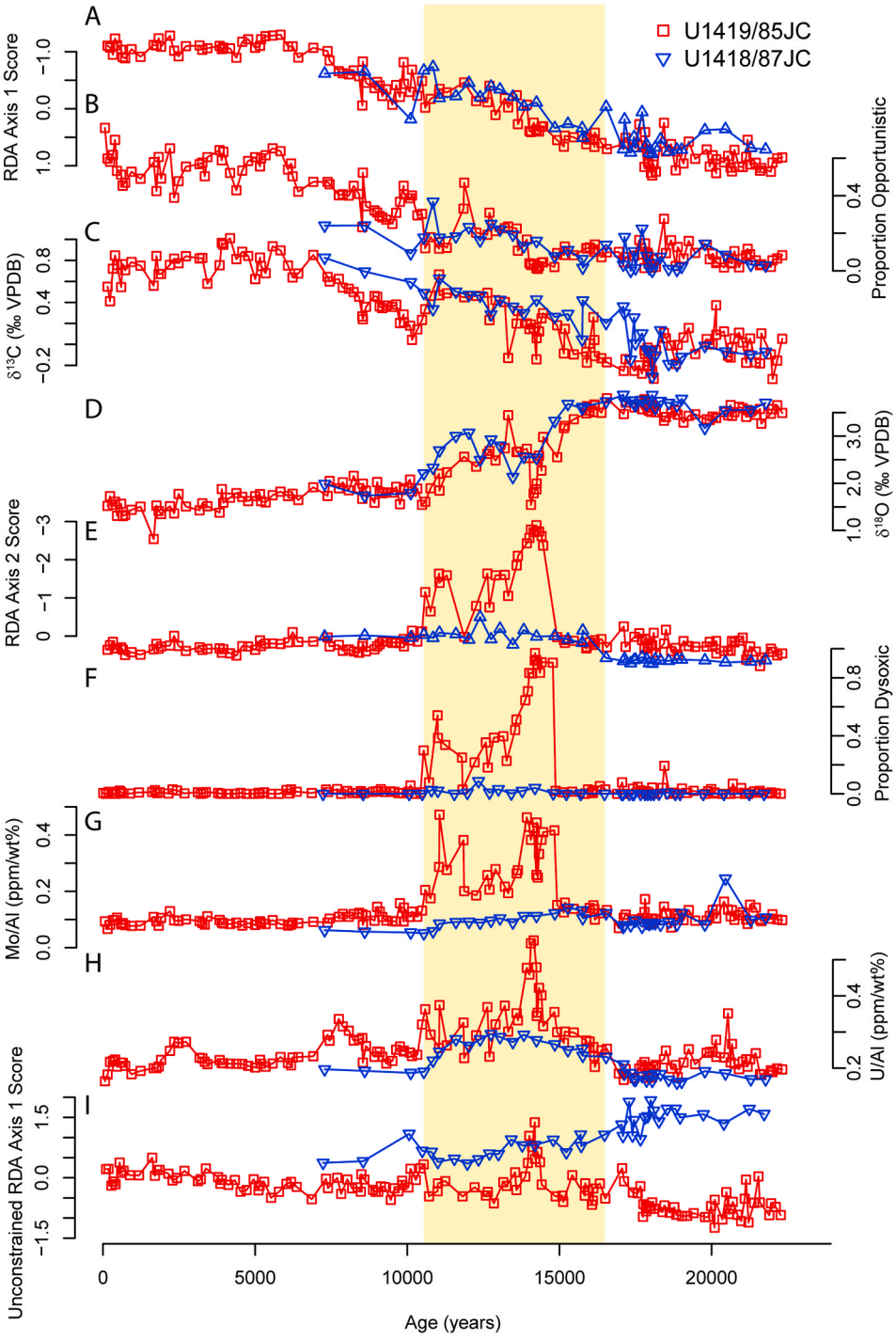

Fig. 2. Environmental proxy and ecological data for the last 22,000 years in the Gulf of Alaska. Red squares = intermediate depth site. Blue triangles = abyssal site. A. RDA Axis 1 scores. B. Proportional abundances of opportunistic benthic foraminifera. C. $\delta^{13}C$ and D. $\delta^{18}O$ were measured on the planktonic foraminifer *Neogloboquadrina pachyderma* (sinistral). E. RDA Axis 2 scores. F. Proportional abundance of benthic foraminifera tolerant of dissolved oxygen concentrations<0.1 ml/L; see Supplemental Table 2 for list of species). G. Mo/Al (ppm/wt%) and H. U/Al (ppm/wt%) measured on sediments. I. The first unconstrained axis from the RDA analysis. Shaded bar indicates the deglacial low-oxygen interval. (For interpretation of the references to colour in this figure legend, the reader is referred to the Web version of this article.)

N. pachyderma are similar at both GoA sites and reflect the transition from glacial to interglacial conditions (Fig. 2). Low planktonic $\delta^{13}C$ with respect to the atmosphere during glacial time may reflect limited gas exchange associated with sea-ice cover and limited nutrient utilization resulting in low carbon export across the subpolar North Pacific based on Pa/Th data (Costa et al., 2018). While the oxygen isotope values of *N. pachyderma* are influenced by multiple factors, including changes in global ice volume, temperature, and regional salinity changes, we use these data here to distinguish the deglacial transition and the differences between glacial and interglacial conditions.

3.2. Responses of benthic faunal composition to environmental change

Across intermediate and abyssal depth study sites, we identified 66 species and 11 taxonomic groups comprised of rare species from the same genus in the >63 μm size fraction. The median sample size is 277 (Interquartile Range (IQR) = 147–417 individuals) at the intermediate-depth site and 272 (IQR = 125–334 individuals) at the abyssal site. The abyssal site generally had fewer foraminifera per gram of sediment than the intermediate-depth site and abyssal faunal densities at ages younger than ~7.4 ka were too low to obtain >50 individuals for analysis (Appendix A).

RDA Axis 1 explains 17.9% of the faunal variation and is strongly constrained by planktonic foraminiferal $\delta^{13}C$ and $\delta^{18}O$ (Fig. 3). Thus, Axis 1 represents faunal patterns associated with glacial-interglacial change at both intermediate and abyssal depths. Axis 1 values trend toward more negative values from the glacial interval to the Holocene such that samples with more positive (glacial and/or colder) $\delta^{18}O$ values have more positive Axis 1 scores and samples with more positive $\delta^{13}C$ values have more negative Axis 1 scores (Fig. 2). Species with the most positive Axis 1 scores include *Cassidulina reniforme* and *Epistominella pacifica*, which are associated with glacial conditions elsewhere in the North Pacific (Ohkushi et al., 2003; see Table S1 for all species scores). *C. reniforme* is also common in modern glacial-proximal settings (Korsun and Hald, 2000) further supporting that samples with high Axis 1 scores were from glacially-influenced environments.

Species with the most negative RDA Axis 1 scores are *Alabaminella wedellensis* and *Epistominella exigua*, both of which are small (typically 63–125 μm), opportunistic taxa associated with fresh phytodetritus and highly seasonal and/or pulsed productivity characteristic of blooms (Smart et al., 1994; Sun et al., 2006, Fig. 2). Other species with moderately negative Axis 1 scores include *Trifarina angulosa*, which is associated with high overall productivity (Hayward et al., 2004), and small (63–125 μm) bolivinids such as *Bolivina decussata* and *Loxostomum minuta*. Based on these faunal associations, we interpret Axis 1 scores as indicating lower export productivity during the glacial maximum interval, transitioning to higher (and pulsed) organic rain to the seafloor in the Holocene, with a relatively smooth transition (i.e., lacking abrupt oscillations during the prominent dysoxic events revealed by the redox-sensitive metals). Axis 1 scores are nearly identical at the intermediate-depth and abyssal sites, which indicates similarity in faunal responses to this climate transition and, thus, suggests that the change from a lower carbon flux glacial system to a higher carbon flux interglacial system occurred at all depths.

Our inference of generally low export productivity during glacial time agrees with findings from Pa/Th data of lower scavenging particle fluxes across the subpolar North Pacific during glacial time (Costa et al., 2018) and nitrogen isotope evidence from the Bering Sea and North Pacific (Worne et al., 2019), but conflicts with interpretations of organic matter and opal content as indications of export productivity (Cartapanis et al., 2016; Ohkushi et al., 2018). The covariance between RDA Axis 1 and $\delta^{13}C$, where high Axis 1 scores correspond to $\delta^{13}C$ values lower than expected from atmospheric equilibrium (Praetorius et al., 2015), further suggests relatively low glacial export productivity and that upper ocean stratification or sea ice cover inhibited gas exchange. Similarly, sedimentary $\delta^{15}N$ from our study site (Addison et al., 2012) supports lower glacial nutrient utilization relative to deglacial or interglacial conditions. These combined analyses of benthic foraminifera faunas from both intermediate and abyssal water depths may more closely capture changes in carbon export to the deep sea floor in the subpolar North Pacific than do organic carbon and opal burial fluxes because they reflect the contemporaneous availability of organic matter at the seafloor rather than what remains after consumption and diagenesis.

RDA Axis 2 explains 9.9% of the faunal variation and is strongly associated with authigenic redox sensitive metals such that samples with more negative Axis 2 scores have higher concentrations of U and Mo (Fig. 3). Thus, we interpret this axis as reflecting faunal differences related to benthic oxygenation that are distinct from faunal changes associated with the glacial-interglacial transition. Consistent with this interpretation, species with the most negative Axis 2 scores tolerate severely dysoxic conditions (as low as <0.1 ml/L O_2) including *Buliminella tenuata*, *Bolivina seminuda*, *Suggrunda eckisi*, and *Takayanagia delicata* (Ohkushi et al., 2013; Erdem and Schonfeld, 2017; Tetard et al., 2017, Figs. 2 and 3). In addition to these dysoxic indicators, species with more moderate negative Axis 2 scores include *Bolivina argentea*, *Bolivina spissa*, and *Bolivina pseudobeyrichi*, which each live in modern suboxic environments and tolerate oxygen levels as low as 0.1–0.5 ml/L (Ohkushi et al., 2013; Tetard et al., 2017). Some of these taxa, including *B. tenuata* (with symbionts), *B. seminuda*, *B. argentea*, and *B. spissa*, respire nitrate instead of oxygen in oxygen minimum zones (Pina-Ochoa et al., 2010; Bernhard et al., 2012; Glock et al., 2019), further supporting that these species are relatively abundant due to extremely low-oxygen conditions.

At the intermediate site, RDA Axis 2 scores become abruptly negative from 14.8 to 14 ka, return to values near zero in the interval 13–12 ka, and are again negative from 11.5 to 10 ka. (Fig. 2). At the abyssal site, variations in Axis 2 are more subdued and species associated with <0.1 ml/L O_2 are rare (Fig. 2). Abyssal Axis 2 scores are more positive than at the intermediate-depth site during the glacial maximum and only become slightly negative during the deglacial transition starting at ~16.5 ka, consistent with the increase in U/Al concentrations. Thus, we infer that the abyssal site was mildly hypoxic, but not sulfidic, during the deglacial transition, consistent with the Mo/Al differences between the sites. We find no evidence for the discrete hypoxic intervals at the abyssal site that were prominent at the intermediate-depth site. While we obtained four constrained axes, the third and fourth constrained axis combined explain less than 4% of the faunal variation and are not discussed.

After accounting for variation associated with the selected environmental constraints, the RDA summarizes the remaining faunal variation on additional ordination axes that are unconstrained by the environmental variables. The first unconstrained RDA axis summarizes 19.1% of the variation and emphasizes the remaining faunal differences between the abyssal and intermediate-depth sites (Fig. 3). On this axis, the sites are most dissimilar during glacial time (the intermediate-depth site is more positive and the abyssal site is more negative during the glacial maximum), but converge in terms of their species compositions during the Holocene (Fig. 2). Species with strong negative scores on the first unconstrained RDA axis include *E. pacifica*, *Uvigerina peregrina*, *Islandiella norcorssi*, *Elphidium clavatum* and *E. exigua*, all of which are more common at the intermediate site than at the abyssal site, especially during the glacial interval. Species with the strongest positive scores include *C. reniforme*, *Nonionella globosa* and *Elphidium batialis*, which all have higher relative abundances at the abyssal site than at the intermediate site. This environmental convergence of the two sites after the glacial maximum interval, irrespective of organic carbon flux or oxygenation, suggests a relaxation of deep stratification across the deglacial transition, consistent with a change between deep haline stratification of the abyssal Pacific during the Last Glacial Maximum, and somewhat more mixed deep Pacific during interglacial time (Adkins, 2013). Additional unconstrained axes (not shown) summarize

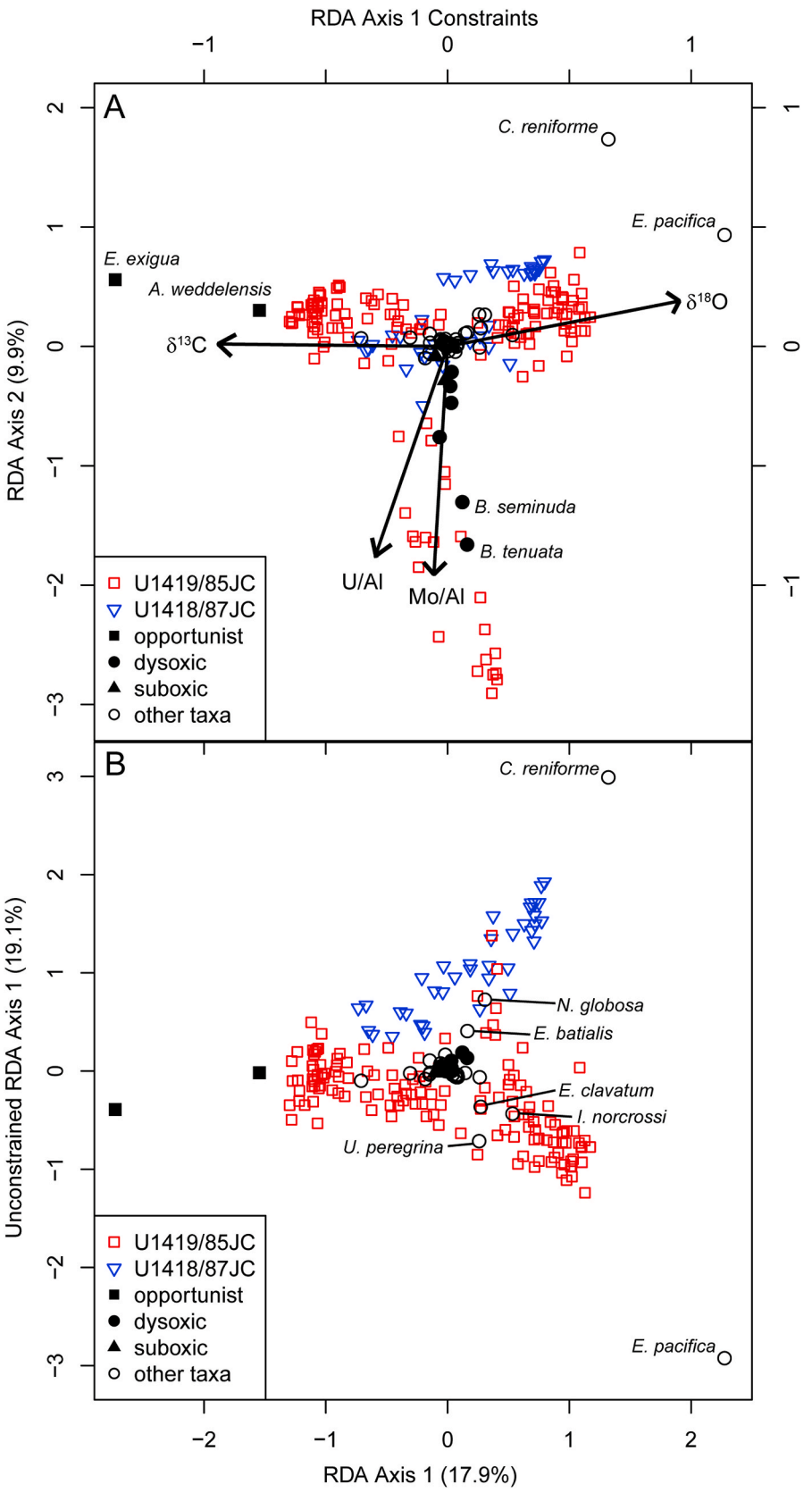

Fig. 3. A. Triplot from distance-based redundancy analysis (RDA) showing position of samples, species, and constraining environmental variables on constrained RDA axis 1 and 2. Arrows denote the direction and relative magnitude of the influence of the constraining variables ($\delta^{13}C$, $\delta^{18}O$, Mo/Al and U/Al) on RDA 1 and 2 rescaled from −1 to 1. Species with the highest and lowest scores on each axis are labeled. B. Biplot of site and species scores for the first constrained and the first unconstrained RDA axes. Species with the highest and lowest scores on the unconstrained axis are labeled. Red squares = intermediate depth site. Blue triangles = abyssal site. Closed black symbols are species coded by known ecological preferences: squares = opportunists, circles = tolerant of dysoxia (<0.1 ml/L O_2), triangles = tolerant of suboxia (0.1–0.5 ml/L O_2). Open black circles are other species. (For interpretation of the references to colour in this figure legend, the reader is referred to the Web version of this article.)

less than 9% of the variation each and are not discussed.

3.3. Ecological metrics indicate changes in ecosystem function

Glacial maximum benthic foraminiferal assemblages have, on average, lower richness (after sample-size standardization to 50 individuals) and evenness than those during the deglacial low-oxygen interval at both the intermediate and abyssal sites (Fig. 4), consistent with a transition from a glacial food-limited ecosystem to a less food-stressed benthic community receiving higher organic matter export (McCallum et al., 2015; Sweetman et al., 2017). After this transition to a benthic community that is not severely food-stressed, richness and evenness remain high despite the lower-oxygen conditions except at the intermediate-depth site during the most extreme low-oxygen conditions at ~14.8–14.2 ka when dysoxic indicator species are dominant.

The overall increased richness and evenness of benthic foraminifera during the deglacial low-oxygen events implies a high-functioning, ecologically healthy benthic foraminiferal community. Previous studies comparing metazoan and foraminiferal responses to environmental change show increases in foraminiferal diversity, evenness, or density while metazoans decline in those metrics (Gooday et al., 2000; Belanger and Villa Rosa Garcia, 2014; Moffitt et al., 2015). Most metazoans are less active or encounter lethal conditions at oxygen levels where foraminifera tolerant of <0.5 ml/L O_2 are abundant (Levin et al., 2000; Vaquer-Sunyer and Duarte, 2008). During the most extreme low-oxygen conditions at the intermediate depth site when benthic foraminiferal diversity declines, metazoans would be restricted from the benthic environment; the presence of laminated sediments at this time (Davies et al., 2011; Penkrot et al., 2018) supports that metazoan activity was indeed reduced during intervals of dysoxia.

4. Conclusions

In this subpolar North Pacific setting, benthic foraminiferal faunal changes demonstrate that glacial retreat is associated with increased organic carbon flux to intermediate and abyssal depths sufficient to affect deep-sea ecosystems. Combined analyses of benthic foraminiferal faunas and of geochemical proxies for redox conditions and glacial-interglacial conditions allow us to separate the confounding signals of organic carbon flux and oxygenation. Unlike other proxies of carbon export that focus on either surface productivity, scavenging particle fluxes, or organic matter burial, benthic foraminiferal faunas are sensitive to organic carbon rain at the seafloor and here illuminate a shift to pulsed organic matter export across the glacial-interglacial transition, an export mode that is most effective at reaching the deep sea. Consistent with respiration-driven dysoxia during the deglacial transition, dysoxic events are prominent in discrete intervals at intermediate depths, but only broad suboxic conditions develop at the abyssal site. Export of organic matter to the sea floor was also great enough at depths up to 3667 m to release benthic foraminiferal communities from glacial food stresses. These results support inferences of increased carbon fluxes during warm intervals of the past, resolving previous disagreement, and demonstrate that the character of organic matter fluxes to deep-sea environments also change with climate. They further support forecasts of future increase in abyssal carbon fluxes following warming and reduction of sea-ice cover. Changes in the character of future productivity may be expected to alter abyssal ecosystems via changes in food availability and respiration at depth.

Declaration of competing interest

The authors declare that they have no known competing financial interests or personal relationships that could have appeared to influence the work reported in this paper.

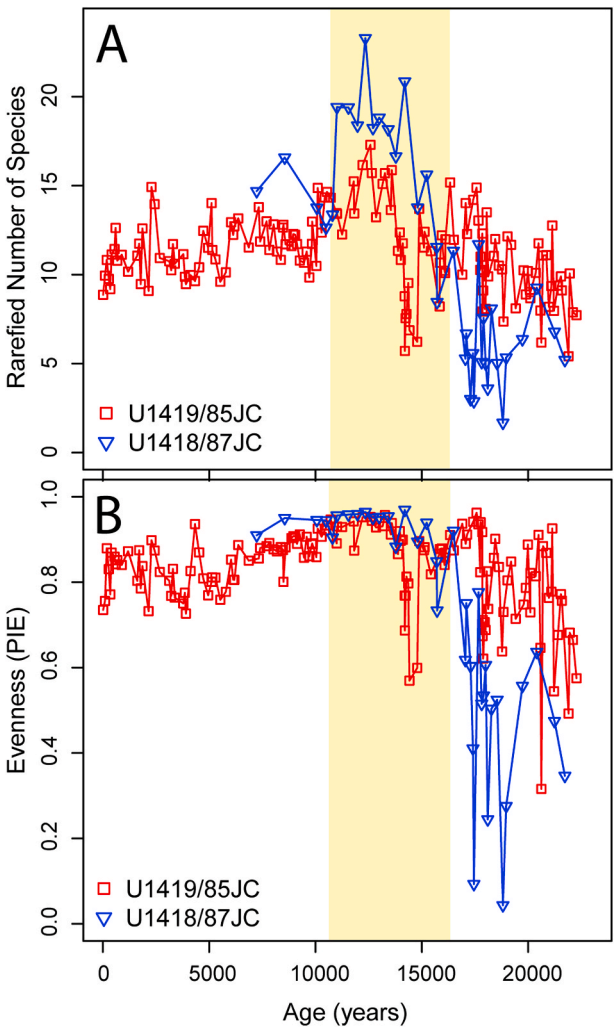

Fig. 4. Ecological metrics for benthic foraminiferal assemblages. A. Species richness calculated as the mean number of species expected in each sample at a sample size of 50 individuals. B. Evenness of benthic foraminiferal assemblages calculated as the probability of interspecific encounter. Red squares = intermediate depth site. Blue triangles = abyssal site. Shaded bar indicates the deglacial low-oxygen interval. (For interpretation of the references to colour in this figure legend, the reader is referred to the Web version of this article.)

Acknowledgements

This work was supported by NSF 1502746 and 1801511 to CLB and NSF 1360894 and 1502754 to ACM. We thank Jesse Muratli from the W. M. Keck Collaboratory for Plasma Spectrometry of Oregon State University for assistance with digesting sediment samples and analyzing metal concentrations. We thank June Padman, Jennifer McKay, and Andy Ross for assistance with stable isotope analyses. Perry Chesebro, Ozlem Orhun, Adrian Sweeney, and Christopher Schiller at SDSMT and Pablo Cavazos at TAMU assisted with fossil sample preparation.

Appendix A. Supplementary data

Supplementary data to this article can be found online at https://doi.org/10.1016/j.dsr.2020.103341.

References

Addison, J.A., Finney, B.P., Dean, W.E., Davies, M.H., Mix, A.C., Stoner, J.S., Jaeger, J. M., 2012. Productivity and sedimentary $\delta^{15}N$ variability for the last 17,000 years along the northern Gulf of Alaska continental slope. Paleoceanography 27.

Adkins, J.F., 2013. The role of deep ocean circulation in setting glacial climates. Paleoceanograph. Paleoclimatol. 28, 539–561.
Arndt, S., Jorgensen, B.B., LaRoe, D.E., Middleburg, J.J., Pancost, R.D., Regnier, P., 2013. Quantifying the degradation of organic matter in marine sediments: A review and synthesis. Earth Sci. Rev. 123, 53–86.
Bapst, D.W., 2012. paleotree: an R package for paleontological and phylogenetic analyses of evolution. Methods Ecol. Evol. 3, 803–807.
Barron, J.A., Bukry, D., Dean, W.E., Addison, J.A., Finney, B., 2009. Paleoceanography of the Gulf of Alaska during the past 15,000 years: results from diatoms, silicoflagellates, and geochemistry. Mar. Micropaleontol. 72, 176–195.
Belanger, C.L., Villa Rosa Garcia, M., 2014. Differential drivers of benthic foraminiferal and molluscan community composition from a multivariate record of early Miocene environmental change. Paleobiology 40, 398–416.
Bernhard, J.M., Casciotti, K.L., McIlvin, M.R., Beaudoin, D.J., Visscher, P.T., Edgcomb, V. P., 2012. Potential importance of physiologically diverse benthic foraminifera in sedimentary nitrate storage and respiration. J. Geophys. Res.: Biogeosciences 117, 1–14.
Bopp, L., Aumont, O., Cadule, P., Alvain, S., Gehlen, M., 2005. Response of diatoms distribution to global warming and potential implications: a global model study. Geophys. Res. Lett. 32, 1–4.
Bopp, L., Resplandy, L., Orr, J.C., Doney, S.C., Dunne, J.P., Gehlen, M., Hallran, P., Heinze, C., Ilyina, T., Séférian, R., Tjiputra, J., Vichi, M., 2013. Multiple stressors of ocean ecosystems in the 21st century: projections with CMIP5 models. Biogeosciences 10, 6225–6245.
Borcard, D., Gillet, F., Legendre, P., 2018. *Numerical Ecology with R*. 452. Springer.
Buzas, M., 1990. Another look at confidence limits for species proportions. J. Paleontol. 64 (5), 842–843.
Cartapanis, O., Bianchi, D., Jaccard, S.L., Galbraith, E.D., 2016. Global pulses of organic carbon burial in deep-sea sediments during glacial maxima. Nat. Commun. 7, 10796.
Cartapanis, O., Tachikawa, K., Bard, E., 2011. Northeastern Pacific oxygen minimum zone variability over the past 70 kyr: impact of biological production and oceanic ventilation. Paleoceanography 26, 1–17.
Chase, Z., Kohfeld, K.E., Matsumoto, K, 2015. Controls on biogenic silica burial in the Southern Ocean. Global Biogeochem. Cycles 29, 1599–1616. https://doi.org/10.1002/2015GB005186.
Costa, K.M., McManus, J.F., Anderson, R.F., 2018. Paleoproductivity and stratification across the subarctic pacific over glacial-interglacial cycles. Paleoceanograph. Paleoclimatol. 33, 914–933.
Davies, M.H., Mix, A.C., Stoner, J.S., Addison, J.A., Jaeger, J., Finney, B., Wiest, J., 2011. The deglacial transition on the southeastern Alaska Margin: meltwater input, sea level rise, marine productivity, and sedimentary anoxia. Paleoceanography 26, 1–18.
Davies-Walczak, M., Mix, A.C., Stoner, J.S., Southon, J.R., Cheseby, M., Xuan, C., 2014. Late glacial to Holocene radiocarbon constraints on North Pacific intermediate water ventilation and deglacial atmospheric CO_2 sources. Earth Planet Sci. Lett. 397, 57–66.
Du, J., Haley, B.A., Mix, A.C., Walczak, M.H., Praetorius, S.K., 2018. Flushing of the deep Pacific Ocean and the deglacial rise of atmospheric CO_2 concentrations. Nat. Geosci. 11, 749–755.
Emerson, S., 2014. Annual net community production and the biological carbon flux in the ocean. Global Biogeochem. Cycles 28, 14–28. https://doi.org/10.1002/2013GB004680.
Erdem, Z., Schönfeld, J., 2017. Pleistocene to Holocene benthic foraminiferal assemblages from the Peruvian continental margin. Palaeontol. Electron. 20 https://doi.org/10.26879/764.
Flombaum, P., Wang, W.L., Primeau, F.W., Martiny, A.C., 2020. Global picophytoplankton niche partitioning predicts overall positive response to ocean warming. Nat. Geosci. 13 (2), 116–120.
Forcino, F.L., Leighton, L.R., Twerdy, P., Cahill, J.F., 2015. Reexamining sample size requirements for multivariate, abundance-based community research: when resources are limited, the research does not have to be. PloS One 10 (6), e0128379.
Glock, N., Roy, A.S., Romero, D., Wein, T., Weissenbach, J., Revsbech, N.P., Høgslund, S., Clemens, D., Sommer, S., Dagan, T., 2019. Metabolic preference of nitrate over oxygen as an electron acceptor in foraminifera from the Peruvian oxygen minimum zone. Proc. Natl. Acad. Sci. U.S.A. 116, 2860–2865.
Gooday, A.J., Bernhard, J.M., Levin, L.A., Suhr, S.B., 2000. Foraminifera in the Arabian Sea oxygen minimum zone and other oxygen-deficient settings: taxonomic composition, diversity, and relation to metazoan faunas. Deep Sea Res. Part II Top. Stud. Oceanogr. 47, 25–54.
Hayward, B.W., Grenfell, H.R., Carter, R., Hayward, J.J., 2004. Benthic foraminiferal proxy evidence for the Neogene palaeoceanographic history of the Southwest Pacific, east of New Zealand. Mar. Geol. 205, 147–184.
Heiberger, R.M., 2018. HH: statistical analysis and data display: heiberger and holland. R package version 3.1. https://CRAN.R-project.org/package=HH, 35.
Honjo, S., Eglinton, T.I., Taylor, C.D., Ulmer, K.M., Sievert, S.M., Bracher, A., German, C. R., Edgcomb, V., Francois, R., Iglesias-Rodriguez, M.D., Van Mooy, B., 2014. Understanding the role of the biological pump in the global carbon cycle: an imperative for ocean science. Oceanography 27, 10–16.
Jochum, K.P., Weis, U., Schwager, B., Stoll, B., Wilson, S.A., Haug, G.H., Andreae, M.O., Enzweiler, J., 2016. Reference values following ISO guidelines for frequently requested rock reference materials. Geostand. Geoanal. Res. 40, 333–350.
Jorissen, F.J., Fontanier, C., Thomas, E., 2007. Paleoceanographical proxies based on deep-sea benthic foraminiferal assemblage characteristics. In: Hillaire–Marcel, C., De Vernal, A. (Eds.), Proxies in Late Cenozoic Paleoceanography. Elsevier, pp. 263–325.
Korsun, S., Hald, M., 2000. Seasonal dynamics of benthic foraminifera in a glacially fed fjord of Svalbard, European Arctic. J. Foraminiferal Res. 30, 251–271.
Lavoie, D., Denman, K.L., Macdonald, R.W., 2010. Effects of future climate change on primary productivity and export fluxes in the Beaufort Sea. J. Geophys. Res. 115. C04018.
Legendre, P., Anderson, M.J., 1999. Distance-based redundancy analysis: testing multispecies responses in multifactorial ecological experiments. Ecol. Monogr. 69, 1–24.
Levin, L.A., Gage, J.D., Martin, C., Lamont, P.A., 2000. Macrobenthic community structure within and beneath the oxygen minimum zone, NW Arabian Sea. Deep Sea Res. Part II 47, 189–226.
Lopes, C., Kucera, M., Mix, A.C., 2015. Climate change decouples oceanic primary and export productivity and organic carbon burial. Proc. Natl. Acad. Sci. U.S.A. 112, 332–335.
McCallum, A.W., Woolley, S., Błażewicz-Paszkowycz, M., Browne, J., Gerken, S., Kloser, R., Poore, G.C., Staples, D., Syme, A., Taylor, J., Walker-Smith, G., 2015. Productivity enhances benthic species richness along an oligotrophic Indian Ocean continental margin. Global Ecol. Biogeogr. 24, 462–471.
McManus, J., Berelson, W.M., Severmann, S., Poulson, R.L., Hammond, D.E., Klinkhammer, G.P., Holm, C., 2006. Molybdenum and uranium geochemistry in continental margin sediments: paleoproxy potential. Geochem. Cosmochim. Acta 70, 4643–4662.
Moffitt, S.E., Hill, T.M., Roopnarine, P.D., Kennett, J.P., 2015. Response of seafloor ecosystems to abrupt global climate change. Proc. Natl. Acad. Sci. U.S.A. 112, 4684–4689.
Morán, X.A.G., López-Urrutia, A., Calvo-Díaz, A., Li, W.K.W., 2010. Increasing importance of small phytoplankton in a warmer ocean. Global Change Biol. 16, 1137–1144.
Muratli, J.M., McManus, J., Mix, A., Chase, Z., 2012. Dissolution of fluoride complexes following microwave-assisted hydrofluoric acid digestion of marine sediments. Talanta 89, 195–200.
Muratli, J., Chase, Z., Mix, A., McManus, J., 2010. Increased glacial-age ventilation of the Chilean margin by antarctic intermediate water. Nat. Geosci. 3, 23–26.
Ohkushi, K., Hata, M., Nemoto, N., 2018. Response of deep-sea benthic foraminifera to paleoproductivity changes on the Shatsky Rise in the Northwestern Pacific Ocean over the last 187 kyr. Paleontol. Res. 22 (4), 326–351.
Ohkushi, K.I., Itaki, T., Nemoto, N., 2003. Last glacial–holocene change in intermediate-water ventilation in the northwestern pacific. Quat. Sci. Rev. 22, 1477–1484.
Ohkushi, K., Kennett, J.P., Zeleski, C.M., Moffitt, S.E., Hill, T.M., Robert, C., Beaufort, L., Behl, R.J., 2013. Quantified intermediate water oxygenation history of the NE Pacific: a new benthic foraminiferal record from Santa Barbara basin. Paleoceanography 28, 453–467.
Oksanen, J., Blanchet, F.G., Friendly, M., Kindt, R., Legendre, P., McGlinn, D., Minchin, P.R., O'Hara, R.B., Simpson, G.L., Solymos, P., Stevens, M.H.H., Szoecs, E., Wagner, H., 2017. Vegan: community Ecology Package. R package version 2.4-4. https://CRAN.R-project.org/package=vegan.
Olsen, A., Key, R.M., van Heuven, S., Lauvset, S.K., Velo, A., Lin, X., Schirnick, C., Kozyr, A., Tanhua, T., Hoppema, M., Jutterström, S., Steinfeldt, R., Jeansson, E., Ishii, M., Pérez, F.F., Suzuki, T., 2016. The Global Ocean Data Analysis Project version 2 (GLODAPv2) – an internally consistent data product for the world ocean. Earth Syst. Sci. Data 8, 297–323.
Penkrot, M.L., Jaeger, J.M., Cowan, E.A., St-Onge, G., LeVay, L., 2018. Multivariate modeling of glacimarine lithostratigraphy combining scanning XRF, multisensory core properties, and CT imagery: IODP Site U1419. Geosphere 14, 1935–1960.
Piña-Ochoa, E., Høgslund, S., Geslin, E., Cedhagen, T., Revsbech, N.P., Nielsen, L.P., Schweizer, M., Jorissen, F., Rysgaard, S., Risgaard-Petersen, N., 2010. Widespread occurrence of nitrate storage and denitrification among Foraminifera and Gromiida. Proc. Natl. Acad. Sci. U.S.A. 107, 1148–1153.
Praetorius, S.K., Mix, A.C., Walczak, M.H., Wolhowe, M.D., Addison, J.A., Prahl, F.G., 2015. North Pacific deglacial hypoxic events linked to abrupt ocean warming. Nature 527, 362–366.
Rogers, A.D., 2015. Environmental change in the deep ocean. Annu. Rev. Environ. Resour. 40, 1–38.
Scott, S., Lyons, T.W., 2012. Contrasting molybdenum cycling and isotopic properties in euxinic versus non-euxinic sediments and sedimentary rocks: refining the paleoproxies. Chem. Geol. 324, 19–27.
Serno, S., Winckler, G., Anderson, R.F., Hayes, C.T., Ren, H., Gersonde, R., Haug, G.H., 2014. Using the natural spatial pattern of marine productivity in the Subarctic North Pacific to evaluate paleoproductivity proxies. Paleoceanography 29, 438–453. https://doi.org/10.1002/2013PA002594.
Smart, C.W., King, S.C., Gooday, A.J., Murray, J.W., Thomas, E., 1994. A benthic foraminiferal proxy of pulsed organic matter paleofluxes. Mar. Micropaleontol. 23, 89–99.
Smith Jr., K.L., Ruhl, H.A., Bett, B.J., Billett, D.S.M., Lampitt, R.S., Kaufmann, R.S., 2009. Climate, carbon cycling, and deep-ocean ecosystems. Proc. Natl. Acad. Sci. U.S.A. 106, 19211–19218.
Smith Jr., K.L., Ruhl, H.A., Huffard, C.L., Messié, M., Kahru, M., 2018. Episodic organic carbon fluxes from surface ocean to abyssal depths during long-term monitoring in NE Pacific. Proc. Natl. Acad. Sci. U.S.A. 115, 12235–12240.
Steinacher, M., Joos, F., Frölicher, T.L., Bopp, L., Cadule, P., Cocco, V., Doney, S.C., Gehlen, M., Lindsay, K., Moore, J.K., Schneider, B., Segschneider, J., 2010. Projected 21st century decrease in marine productivity: a multi-model analysis. Biogeosciences 7, 979–1005.
Sun, X., Corliss, B.H., Brown, C.W., Showers, W.J., 2006. The effect of primary productivity and seasonality on the distribution of deep-sea benthic foraminifera in the North Atlantic. Deep Sea Res. Oceanogr. Res. Pap. 53, 28–47.
Sweetman, A.K., Thurber, A.R., Smith, C.R., Levin, L.A., Mora, C., Wei, C.L., Gooday, A. J., Jones, D.O., Rex, M., Yasuhara, M., Ingels, J., Ruhl, H.A., Frieder, C.A.,

Danovaro, R., Würzberg, L., Baco, A., Grupe, B.M., Pasulka, A., Meyer, K.S., Dunlop, K.M., Henry, L.-A., Roberts, M.J., 2017. Major impacts of climate change on deep-sea benthic ecosystems. Elementa: Sci. Anthropocene. 5.

Tetard, M., Licari, L., Beaufort, L., 2017. Oxygen history off Baja California over the last 80 kyr: a new foraminiferal-based record. Paleoceanography 32, 246–264.

Tribovillard, N., Algeo, T.J., Lyons, T., Riboulleau, A., 2006. Trace metals as paleoredox and paleoproductivity proxies: an update. Chem. Geol. 232, 12–32.

Vaquer-Sunyer, R., Duarte, C.M., 2008. Thresholds of hypoxia for marine biodiversity. Proc. Natl. Acad. Sci. U.S.A. 105, 15452–15457.

Worne, S., Kender, S., Swann, G.E., Leng, M.J., Ravelo, A.C., 2019. Coupled climate and subarctic Pacific nutrient upwelling over the last 850,000 years. Earth Planet Sci. Lett. 522, 87–97.

Zheng, Y., Anderson, R.F., van Geen, A., Kuwabara, J., 2000. Authigenic molybdenum formation in marine sediments: a link to pore water sulfide in the Santa Barbara Basin. Geochem. Cosmochim. Acta 64 (24), 4165–4178.